Research Square

Preprints are preliminary reports that have not undergone peer review.
They should not be considered conclusive, used to inform clinical practice,
or referenced by the media as validated information.

Specific Interactions Between The Alkaline Protease of *P. Aeruginosa* And Its Natural Peptide Inhibitor: *Ab Initio* Molecular Simulations

Ryosuke Saito
Toyohashi University of Technology: Toyohashi Gijutsu Kagaku Daigaku
Kyohei Imai
Toyohashi University of Technology: Toyohashi Gijutsu Kagaku Daigaku
Shohei Yamamoto
Toyohashi University of Technology: Toyohashi Gijutsu Kagaku Daigaku
Takuya Ezawa
Toyohashi University of Technology: Toyohashi Gijutsu Kagaku Daigaku
Satoshi Sugiyama
Toyohashi University of Technology: Toyohashi Gijutsu Kagaku Daigaku
Linn Samira Mari Evenseth
UiT The Arctic University of Norway: UiT Norges arktiske universitet
Ingebrigt Sylte
UiT The Arctic University of Norway: UiT Norges arktiske universitet
Noriyuki Kurita (kurita@cs.tut.ac.jp)
Toyohashi University of Technology

Research Article

Keywords: Protein–protein interactions, Metalloprotease, Protonation, Molecular simulation, Fragment molecular orbital, Drug design

Posted Date: June 14th, 2021

DOI: https://doi.org/10.21203/rs.3.rs-523800/v1

License: This work is licensed under a Creative Commons Attribution 4.0 International License.
Read Full License

Version of Record: A version of this preprint was published at Journal of Molecular Modeling on December 16th, 2021. See the published version at https://doi.org/10.1007/s00894-021-04991-y.

Abstract

Alkaline protease aeruginolysin (APR) is an important virulence factor in the evasion of the immune system by *Pseudomonas aeruginosa (P. aeruginosa)*. The *P. aeruginosa* genome also encodes the highly potent and specific APR peptide inhibitor (APRin). However, the structural reason for the significant inhibition has not been revealed. Using *ab initio* molecular simulations, we here investigated the specific interactions between APR and APRin to elucidate which amino acid residues of APRin and APR contribute strongest to the inhibition. Since APR has a Zn ion at the ligand-binding site, and histidine and glutamic acid residues are coordinated with Zn, it is essential to precisely describe these coordination bonds to elucidate the specific interactions between APR and APRin. Therefore, we employed the *ab initio* fragment molecular orbital method to investigate the specific interactions at an electronic level. The results revealed that Ser1 and Ser2 at the N-terminal of APRin significantly contribute to the binding between APRin and APR. In particular, Ser1 binds strongly to Zn as well as to the sidechains of Hid176, Hid180, and Hid186 in APR. This is the main reason for the strong interaction between APR and APRin. The results also elucidated significant contributions of the positively charged Arg83 and Arg90 residues of APRin to the binding with APR. These findings may provide information useful for the design of novel small agents as potent APR inhibitors.

Introduction

In the treatment of bacterial infectious diseases, many types of antimicrobial agents have been widely used, acting directly on bacteria and inhibiting their growth. However, prolonged use of the same agent at high concentrations increases the risk of the emergence of novel bacteria with antimicrobial resistance against the agent. These drug-resistant strains of bacteria have become extremely dangerous for human beings, as cautioned by the World Health Organization (WHO): “Antimicrobial resistance: no action today, no cure tomorrow” [1]. Therefore, to inhibit infections by drug-resistant bacteria, there is an urgent need to develop novel antimicrobial agents that have different modes of behavior to bacteria and a low risk of causing drug-resistance [2].

Pseudomonas aeruginosa (P. aeruginosa) occurs widely in nature and is a major source of both community-acquired and hospital-acquired infections among human beings. *P. aeruginosa* secretes various virulence factors, such as elastase and alkaline proteases. Among these alkaline proteases, aeruginolysin (APR) is an important virulence factor in the evasion of the immune system by *P. aeruginosa* [3, 4]. The *P. aeruginosa* genome also encodes a natural peptide APR inhibitor (APRin) [5]. To suppress the growth of *P. aeruginosa*, various truncated APRin analogous and analogous based on the homology with naturally occurring peptide inhibitors of alkaline proteases from other bacterial species were constructed [5, 6]. However, no small molecular inhibitor is known for APR. Since APR inhibitors do not act on *P. aeruginosa* directly, it is expected that they can help significantly reduce the risk of producing drug-resistant *P. aeruginosa*.

In a previous crystal structure analysis [7], the 3D structures of APR and its natural peptide inhibitor APRin were elucidated. As shown in Figure S1 in the Supplementary Information (SI), APR has a Zn ion at the ligand-binding site, and the Zn ion significantly contributes to the specific interactions between APR and its inhibitor. APRin (Figure S1b) is composed of 105 amino acid residues, and its equilibrium dissociation constant (K_D) against APR is 4 pM [5]. This value is significantly lower than corresponding values of the naturally occurring inhibitors of the alkaline proteases of *Erwinia chrysanthemi* (1–10 μM) [8] and *Serratia marcescens* (0.7 μM) [9]. Therefore, APRin is expected to be a more potent inhibitor against APR than existing ones. In addition, it has been revealed that the N-terminal site of APRin is important for the strong binding between APRin and APR [5, 6]. However, the reason for the strong binding of APRin to APR has not been elucidated. This is acting as a bottleneck to the further development of novel small agents based on important amino acid residues contained in the APRin peptide, which should have significant inhibitory effects against APR.

In the present study, we investigate the specific interactions between the APRin and APR residues to determine which residues in APRin contribute to its binding to APR, with the aim of eventually proposing novel agents as potent inhibitors against APR in the future. Since APR involves a Zn ion in the ligand-binding pocket, and Zn significantly contributes to the binding between APR and APRin, we carefully considered the protonation states of the residues existing around the Zn ion using molecular simulations based on molecular mechanics (MM) and the fragment molecular orbital (FMO) methods. First, we precisely determined the preferable protonation states of histidine (His) and glutamic acid (Glu) residues located around the Zn ion of APR using MM optimizations. Subsequently, the electronic states of the optimized structure for the APR + APRin complex were investigated by the *ab initio* FMO method. Based on the results obtained from the FMO calculations, we were able to reveal which residues of APR and APRin significantly contribute to the specific interactions between APR and APRin. Based on this information, we give a preliminary proposal of small peptide agents to be used as potent inhibitors against APR.

Details Of Ab Initio Molecular Simulations

2.1. Determination of His and Glu protonation states and APR and APRin peptide terminations

In the present study, we employed the PDB structure of the APR + APRin complex (PDB ID: 1JIW) [7]. As this structure contains no information on the positions of hydrogen atoms, to conduct realistic molecular simulations, it is necessary to add hydrogen atoms at the appropriate positions of the APR + APRin complex. In fact, if hydrogen atoms are not added to the appropriate positions of the target protein, the results simulated will not be realistic and cannot be compared with results obtained by experiments, as shown in our previous study on the specific interactions between a vitamin-D receptor and its ligands [10]. His and Glu may have different types of protonation state depending on the protein structure. Therefore, we carefully determined their protonation states in the APR + APRin complex.

First, we gave assignments to the protonation states of eight His residues in the APR + APRin complex based on the pKa values predicted by the PROPKA 3.0 program [11, 12]. His residues that had a pKa value greater than 6 and were located on the surface of the complex were assigned the Hip^+ protonation, whereas His residues with a lower pKa value located inside the complex were assigned the Hid or Hie protonation. The chemical structures of His residue with these protonation states are shown in Figure S2 (see SI). Since His residues located inside a protein can be in either the Hid or Hie state depending on the structure of the surrounding residues, we gave assignments to the protonation state considering the steric hindrance to the surrounding residues of APR and APRin.

The pKa values, protonation states, and positions of the His residues in the APR + APRin complex are listed in Table S1 (see SI). As the His14, His27, His110, and His452 of APR and His27 of APRin have relatively high pKa values and are located on the surface of APR or APRin, these His residues were assigned the Hip^+ protonation state. In contrast, His176, His180, and His186 are coordinated with the Zn ion in APR, as shown in Fig. 1. It should be noted that the Zn ion is coordinated with the nitrogen atoms at the ε-site of the imidazole ring of these His residues, and that these coordination bonds do not form if a proton is added to the ε-site. Accordingly, Fig. 1 clarifies that these His residues should possess Hid protonation states. As described below, the protonation states of these His residues have a significant influence on the structure and the electronic properties around the Zn ion of the active site of APR.

Next, we determined the protonation states of the Glu residues in the APR + APRin complex. Glu can have three types of protonation states, as defined in Figure S3 (Glu^-, Glh-1, and Glh-2; see SI). Glu^- is a non-protonated state with a negative charge, whereas Glh-1 and Glh-2 are protonated states, in which one of the oxygen atoms of the carboxylate group of the Glu^- sidechain is protonated. In the APR + APRin complex, Glu177 exists near the Zn ion, and its protonation state can have a remarkable influence on the structure around the Zn ion. Therefore, we optimized the APR + APRin structure using the classical MM method based on an Assisted Model Building with Energy Refinement (AMBER) force field [13], considering the three different Glu177 protonation states. The optimized structures were compared with the PDB structure to determine the structure with the smallest deviation from the PDB structure of the APR + APRin complex. This structure was considered the most realistic one with the preferable Glu177 protonation state.

APRin has a disulfide bond between its cysteine (Cys) residues. In particular, the sulfur atoms of Cys29 and Cys52 lose their hydrogen atoms to form the disulfide bond. Thus, we altered these Cys residues into deprotonated states and added a connection between the deprotonated Cys residues. This disulfide bond is considered to be important for maintaining the conformation of APRin.

When using the tleap command of AMBER18 [13], the N- and C-terminals of an amino acid peptide are usually terminated by the NH_3^+ and COO^- groups, respectively, as shown in Figure S4b (see SI). However, a previous experiment [7] revealed that the Ser residue at the N-terminal of APRin is coordinated with the Zn ion of APR and significantly contributes to the interaction between APR and APRin. If the N-terminal of APRin has a charged NH_3^+ group, there is the possibility that the repulsive electrostatic interaction

between the N-terminal of APRin and the Zn ion of APR will be massively overestimated. It is likely that the non-charged NH_2 and COOH groups (Figure S4a) at the N- and C-terminals of APR and APRin would be more appropriate for describing the interaction between ARP and APRin. However, there is no AMBER force field for these non-charged groups. Therefore, we additionally employed the acetyl (Ace) and the N-methyl (Nme) groups to terminate the N- and C-terminals of the APR and APRin peptides, respectively, as shown in Figure S4c (see SI). From the comparison of the MM optimized structures with the PDB one, we determined preferable structures of the N- and C-terminals.

2.2. Optimization of APR + APRin structure by the MM method

The structure of the APR + APRin complex was fully optimized in water using the classical MM and molecular dynamics simulation program AMBER18 [13]. To properly consider the solvation effect on the complex, we added the solvating water molecules in an 8-Å layer around the complex. The total number of water molecules considered was approximately 3,700. In the MM optimizations, the FF14SB force field [14] and TIP3P model [15] were used for the APR/APRin and the water molecules, respectively. The threshold value of the energy gradient for convergence in the MM optimization was set to 0.0001 kcal/mol/Å.

With the aim of obtaining an optimum solvated structure that was not significantly deformed from the PDB structure, we here employed the following steps to optimize the structure of the APR + APRin complex in explicit water molecules:

(1) optimization of only the terminal groups of APR and APRin;
(2) optimization of only the hydrogen atoms added to the PDB structure;
(3) addition of solvating water molecules and optimization of these as well as the hydrogen atoms of APR and APRin;
(4) full optimization of the APR + APRin complex including the crystal and solvating water molecules.

2.3. FMO calculations for the optimized structure of the APR + APRin complex

To elucidate the specific interactions between APR and APRin, the electronic properties for the optimized structure of the APR + APRin complex were investigated using the *ab initio* FMO method [16]. We employed 592 crystal water molecules detected in a previous X-ray analysis [7] to explore their roles in the interactions between APR and APRin. In the FMO calculations, the target molecule is divided into units, each of which is called a “fragment,” and the electronic properties of the target molecule are estimated based on the electronic properties of the monomers and the dimers of the fragments. The specific interactions between the fragments can be investigated based on the interaction energies obtained by the FMO calculations. In the present FMO calculations, each residue of APR and APRin and each water molecule were considered as separate fragments, as this fragmentation would allow us to evaluate the interaction energies between the residues of the APR and APRin peptides under the effect of crystal water molecules. It should be noted that the Zn ion and the Hid176, Hid180, and Hid186 residues are coordinated, as shown in Fig. 1. Therefore, these Hid residues were considered as part of the same

fragment as the Zn ion to precisely describe the coordination bonds among them. Further, the Cys29 and Cys52 of APRin were included in the same fragment, as these Cys residues form a disulfide bond.

The FMO calculation program ABINIT-MP Ver.6.0 [17] was used in the present study. The *ab initio* MP2/6-31G method [18, 19] of FMO was employed to accurately investigate the π–π stacking, NH–π, and CH–π interactions as well as the hydrogen-bonding and electrostatic interactions between the residues of APR and APRin. In addition, to reveal which residues contribute to the binding, we investigated the inter fragment interaction energies (IFIEs) [20] obtained in the FMO calculations.

Results And Discussion

3.1. Protonation state of Glu177 and N- and C-terminals of APR + APRin

As Glu177 exists near the Zn ion of APR and has a significant effect on APR activity, its protonation state had to be determined in an appropriate manner. Thus, we considered the different protonation states (Figure S3 in the SI) of Glu177 and optimized the structure of the solvated APR + APRin complex using the MM method. The obtained structures were compared with the PDB structure, and the most appropriate protonation state of Glu177 that did the best job reproducing the PDB structure of the APR + APRin complex was determined.

In the PDB structure [7] of the APR + APRin complex, the Glu177 of APR, the catalytic base of the HEXXH motif, forms a hydrogen bond with the Ser2 of APRin. In our optimized complex structures, there is no hydrogen bond between Glu177 and Ser2 when Glu177 has a Glu^- or Glh-2 protonation state, as shown in Fig. 2a and c, respectively. At the same time, the oxygen atom of the Glu177 sidechain is separated from the oxygen atom of the OH group of the Ser2 sidechain. Notably, a crystal water molecule bridging the Ser2 and Thr173 of APR plays an important role in determining the direction of the OH group. In contrast, Fig. 2b reveals that the OH group of the Glu177 sidechain forms a hydrogen bond with the oxygen atom of Ser2 when Glu177 is in the Glh-1 protonation state. This hydrogen bond (Fig. 2b) is comparable to that in the PDB structure [7]. Consequently, Fig. 2 demonstrates that Glh-1 is the most preferable protonation state for the Glu177 of APR in the X-ray structure.

In the PDB structure [7] of the APR + APRin complex, the OH group of the Ser1 sidechain as well as the backbone N atom of the Ser1 located at the N-terminal of APRin are directly coordinated with the Zn ion of APR, as shown in Fig. 3a. Therefore, the structures of the N- and C-terminals of APRin as well as APR are likely to have a significant influence on the interaction between APR and APRin. Thus, we considered different types of terminal structures for both the APR and APRin peptides to determine the most preferable structure.

At first, we assigned the NH_3^+ and COO^- structures to the N- and C-terminals, respectively, and the APR + APRin complex structure was optimized using the MM method. As shown in Fig. 3b, the structure around the Zn ion was altered significantly from the PDB structure due to the repulsive electrostatic interaction

between the NH_3^+ group of APRin and the Zn ion. Accordingly, it was revealed that the altered NH_3^+ and COO^- structures are not suitable for reproducing the PDB structure [7] of the APR + APRin complex.

Next, we assigned the Ace and Nme structures to the N- and C-terminals, respectively, as shown in Figure S4c in the SI. The optimized structure around the Zn ion is shown in Fig. 3c. The oxygen atom of the Ace group coordinated directly to the Zn ion at 1.84 Å distance, and the distance between the N atom of the Ser1 main chain and the Zn ion was elongated to 3.6 Å, resulting in significant deformation from the PDB structure (Fig. 3a). Therefore, the Ace group was found to be unsuitable for the N-terminal structure of APPin.

The results indicated that the NH_2 group remained as the only choice for the N-terminal structure of APRin. However, a force field for the NH_2 terminal was not prepared among the AMBER force fields. Therefore, we added hydrogen atoms and solvating water molecules to the PDB structure of the APR + APRin complex and optimized only the positions of the hydrogen atoms and the water molecules using the AMBER18-MM method, under the assumption that the N- and C-terminal structures were the NH_3^+ and COO^- groups, respectively. In the optimized structure, the NH_3^+ and the COO^- of APR and APRin were changed into NH_2 and COOH, respectively. The specific interactions between APR and APRin for this structure were investigated at an electronic level using the *ab initio* FMO method.

3.2. Specific interactions between APR and APRin

To determine the residues of APRin that are the main contribution to the specific binding between APRin and APR, we first investigated the total IFIEs of each APRin residue with all APR residues. As shown in Fig. 4, the Ser1 and Ser2 at the N-terminal of APRin as well as the charged Arg83 and Arg90 residues have large attractive total IFIEs. In particular, Ser1 strongly interacts with the APR residues.

In the present FMO calculations, we considered crystal water molecules explicitly and evaluated the electronic properties of the APR + APRin complex in a vacuum. As a result, the electrostatic interactions between the APR and APRin residues were overestimated, as indicated in Fig. 4. It is expected that this overestimation would be improved by considering a continuum solvation model. However, the trend of the IFIEs is likely to not change even when the continuum solvation model is employed.

The previous experiments [5, 7] revealed that the Ser1 backbone carbonyl of APRin interacts with the catalytic Zn, while the Ser2 side chain of APRin forms a hydrogen bond to the carboxyl end of the catalytic Glu177 of APR. Our present FMO results (Fig. 4), which indicate the significant contribution of the Ser1 and Ser2 residues to the binding to APR, are comparable to these experimental results.

To elucidate the reason for the high attractive interaction energy between Ser1 and the APR residues, we investigated the IFIEs between Ser1 and each of the APR residues. As shown in Fig. 5a, Ser1 interacts very strongly with the Zn group of APR and has no significant interaction with the other APR residues. In fact, as indicated in Fig. 5b, the OH group of the Ser1 sidechain interacts electrostatically with the

imidazole ring of APR Hid186, and the N atom of the NH_2 group at the N-terminal of Ser1 is directly coordinated at 2.33 Å to the Zn ion of APR. In addition, one of the H atoms of the terminal NH_2 group of Ser1 forms a hydrogen bond with the imidazole ring of Hid180, whereas the other H atom interacts electrostatically with the imidazole ring of Hid176. Accordingly, Fig. 5b indicates that the N-terminal part of APRin is important for the strong binding between APRin and the Zn group of APR.

Further, the Ser2 of APRin interacts with the APR residues in a similar way to Ser1. As shown in Fig. 6a, it interacts strongly with the Zn group. However, the size of IFIE for Ser2 is approximately one-fifth of that for Ser1. This difference in the IFIEs results in a larger total IFIE for Ser1 than for Ser2, as shown in Fig. 4. The oxygen atom of the main chain between Ser2 and Ser1 is strongly coordinated to the Zn ion, as shown in Fig. 6b, whereas no other interaction was found between Ser2 and the APR residues. As a result, the interaction between Ser2 and APR is significantly weaker than that of Ser1.

Figure 4 also elucidated that the Arg83 and Arg90 residues, which exist far from the N-terminal of APRin, interact strongly with the APR residues. These APRin residues are positively charged and can interact electrostatically with the charged residues of APR. To explain their strong interactions, we investigated the IFIEs among Arg83/Arg90 and each of the APR residues. As shown in Fig. 7a, Arg83 interacts with many APR residues in an attractive or repulsive manner. These interactions are mainly caused by the electrostatic interactions between the charged Arg83 and the charged residues of APR. In particular, Arg83 interacts strongly with the negatively charged Asp196 and Glu218 residues of APR. In fact, the NH_2^+ group of the Arg83 sidechain forms a hydrogen bond (2.55 Å) with the COO^- group of the Asp196 sidechain, as shown in Fig. 7b. In addition, Arg83 interacts electrostatically with the COO^- group of the Glu218 sidechain at a 5.26-Å distance.

The Arg90 of APRin also interacts with many APR residues, as shown in Fig. 8a. Among the APR residues, negatively charged Asp196, Asp201, and Glu218 interact strongly with the positively charged Arg90 of APRin. Although these residues exist a significant distance from Arg90, as shown in Fig. 8b, long-range electrostatic interactions occur via the charged groups of these charged residues. Accordingly, our present *ab initio* FMO calculations elucidate that the charged residues of APR contribute significantly to the specific interactions between APR and the charged Arg83 and Arg90 residues of APRin, as indicated in Figs. 7 and 8.

It was elucidated from the present FMO study that the Ser1, Ser2, Arg83, and Arg90 of APRin are the main contributors to the interactions between APRin and APR. In particular, Fig. 4 indicates that the Ser1 at the N-terminal of APRin interacts strongly with the Zn group of APR, playing an important role in the interaction. In a previous experiment [5], the six residues at the N-terminal of APRin were found to be necessary to the inhibitory effect of APRin against APR. Our present FMO calculations highlight that among the six residues, Ser1 and Ser2 are particularly important for strong binding to APR. In addition, the charged Arg83 and Arg90 residues of APRin were found to contribute to the binding between APRin and APR. These facts became evident after investigating the electronic properties of the APR + APRin complex using the *ab initio* FMO method.

The main aim of our work is to obtain small molecular inhibitors of APR, and the present FMO results are important guidelines for that. Based on the total IFIEs for each of the APRin residues shown in Fig. 4, it is possible to suggest a number of small peptides as putative inhibitors. A dipeptide consisting of Ser1 and Ser2 would be the smallest possible peptide inhibitor. However, a previous structural and mutational study [6] revealed that a peptide consisting of the first five N-terminal residues (Ser1-Ser2-Lue3-Ile4-Leu5) of APRin did not inhibit the APR activity, indicating that the peptide did not obtain a proper orientation at the APR active site for inhibiting the enzyme. This result indicates the importance of the APRin main body for guiding the N-terminus to the active-site cleft of APR. In the present study, the positively charged Arg83 and Arg90 residues of APRin were found to interact strongly with many charged residues of APR, as shown in Figs. 7 and 8. Therefore, there is a possibility that these residues may act as anchor sites for proper orientation of the N-terminal residues within the APR active site. Studies are now underway to optimize the structures of our proposed molecules and investigate their binding properties to APR. The results will be published elsewhere.

Conclusions

In the present molecular simulations based on the classical MM and *ab initio* FMO methods, we investigated the specific interactions between APR and its natural peptide inhibitor (APRin) to elucidate which residues of APRin and APR contribute to their interactions at an electronic level. Since APR contains a Zn ion near the ligand-binding site, we precisely determined the protonation states of His and Glu residues located around the Zn ion. In addition, as the N-terminal of APRin contributes significantly to the binding to APR, we considered various structures for the N- and C-terminals of the APRin and APR peptides and determined the most preferable structure via MM optimizations. Finally, the electronic properties of the optimized APR + APRin complex structure were investigated by the *ab initio* FMO calculations. The results indicate that the Ser1 and Ser2 at the N-terminal of APRin as well as the positively charged residues (Arg83 and Arg90) of APRin contribute significantly to the binding between APRin and APR. In particular, Ser1 binds strongly to both the Zn ion and the Hid residues coordinated to the Zn. We went on to propose novel peptides including Ser1, Ser2, Arg83, and Arg90 residues of APRin as potent APR inhibitors.

Declarations

Acknowledgments

This collaboration study was carried out under the official agreement regarding international collaboration studies and the student exchange program between Toyohashi University of Technology and UiT–The Arctic University of Norway. The study was also supported by the international internship program of the Japan Student Services Organization (JASSO).

Author declarations

Funding:

This study was supported by the Nitto Foundation and the Northern Norway Health Authorities (Helse Nord) (grant number HNF 1514–20).

Conflicts of interest/Competing interests:

The authors declare that there is no conflict/competing of interests.

Availability of data and material: N/A

Code availability: N/A

Authors' contributions:

R.S., K.I., S.Y., T.E, and S.S. contributed to doing molecular simulations and analysing the results. L.S.M.E. and I.S. contributed to the discussions of the simulated results. N.K. contributed to planning the study, the discussions, and writing the manuscript.

References

1. “WHO | World Health Day – 7 April 2011,” WHO, 2013
2. Smith P, Romesberg F (2007) Combating bacteria and drug resistance by inhibiting mechanisms of persistence and adaptation. Nat Chem Biol 3:549–556
3. Matheson NR, Potempa J, Travis J (2006) Interaction of a novel form of pseudomonas aeruginosa alkaline protease (aeruginolysin) with interleukin-6 and interleukin-8. Biol Chem 387:911–915
4. Guyot N, Bergsson G, Butler MW, Greene CM, Weldon S, Kessler E, Levine RL, O'Neill SJ, Taggart CC, McElvaney NG (2010) Functional study of elafin cleaved by pseudomonas aeruginosa metalloproteinases. Biol Chem 391:705–716
5. Feltzer RE, Gray RD, Dean WL, Pierce WM (2000) Alkaline proteinase inhibitor of pseudomonas aeruginosa; interaction of native and n-terminally truncated inhibitor proteins with pseudomonas metalloproteinases. J Biol Chem 275:21002–21009
6. Bardoel BW, van Kessel KM, van Strijp JG, Milder FJ (2012) Inhibition of *Pseudomonas aeruginosa* virulence: Characterization of the AprA–AprI interface and species selectivity. J Mol Biol 415:573–583
7. Hege T, Feltzer RE, Gray RD, Baumann U (2001) Crystal structure of a complex between pseudomonas aeruginosa alkaline protease and its cognate inhibitor. J Biol Chem 276:35087–35092
8. Le´toffe´S, Delepelaire P, Wandersman C (1989) Characterization of a protein inhibitor of extracellular proteases produced by Erwinia chrysanthemi. Mol Microbiol 3:79–86

9. Bae KH, Kim IC, Kim KS, Shin YC, Byun SM (1998) The Leu-3 residue of Serratia marcescens metalloprotease inhibitor is important in inhibitory activity and binding with Serratia marcescens metalloprotease. Arch Biochem Biophys 352:37–43
10. Terauchi Y, Suzuki R, Takeda R, Kobayashi I, Kittaka A, Takimoto-Kamimura M, Kurita N (2019) Ligand chirality can affect histidine protonation of vitamin-D receptor: Ab initio molecular orbital calculations in water. J Steroid Biochem Mol Biol 186:89–95
11. Søndergaard CR, Olsson MHM, Rostkowski M, Jensen JH (2011) Improved treatment of ligands and coupling effects in empirical calculation and rationalization of pKa values. J Chem Theory Comput 7:2284–2295
12. Olsson MHM, Søndergaard CR, Rostkowski M, Jensen JH (2011) PROPKA3: Consistent treatment of internal and surface residues in empirical pKa predictions. J Chem Theory Comput 7:525–537
13. Kollman PA et al (2018) AMBER 2018. University of California, San Francisco
14. Maier JA, Martinez C, Kasavajhala K, Wickstrom L, Hauser KE, Simmerling C (2015) FF14SB: Improving the accuracy of protein side chain and backbone parameters from ff99SB. J Chem Theory Comput 11:3696–3713
15. Jorgensen WL, Chandrasekhar J, Madura JD, Impey RW, Klein ML (1983) Comparison of simple potential functions for simulating liquid water. J Chem Phys 79:926–935
16. Fedorov DG, Nagata T, Kitaura K (2012) Exploring chemistry with the fragment molecular orbital method. Phys Chem Chem Phys 14:7562–7577
17. Mochizuki Y, Yamashita K, Nakano T, Okiyama Y, Fukuzawa K, Taguchi N, Tanaka S (2011) Higher-order correlated calculations based on fragment molecular orbital scheme. Theor Chem Acc 130:515–530
18. Mochizuki Y, Nakano T, Koikegami S, Tanimori S, Abe Y, Nagashima U, Kitaura K (2004) A parallelized integral-direct second-order Møller-Plesset perturbation theory method with a fragment molecular orbital scheme. Theor Chem Acc 112:442–452
19. Mochizuki Y, Koikegami S, Nakano T, Amari S, Kitaura K (2004) Large scale MP2 calculations with fragment molecular orbital scheme. Chem Phys Lett 396:473–479
20. Fukuzawa K, Komeiji Y, Mochizuki Y, Kato A, Nakano T, Tanaka S (2006) Intra- and intermolecular interactions between cyclic-AMP receptor protein and DNA: Ab initio fragment molecular orbital study. J Comput Chem 27:948–960

Figures

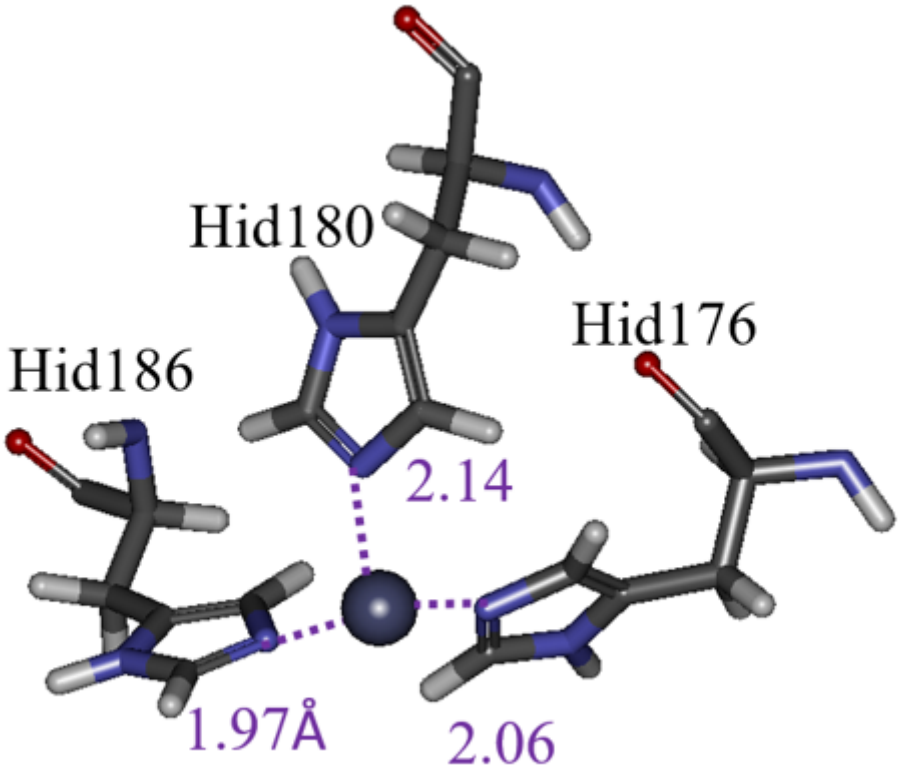

Figure 1

Coordination bonds between the Zn ion and three His residues in APR (PDB ID: 1JIW) [7]. It is noted that Zn is coordinated with the nitrogen atoms at the ε-site of the imidazole ring of these His residues, resulting in the Hid protonation states.

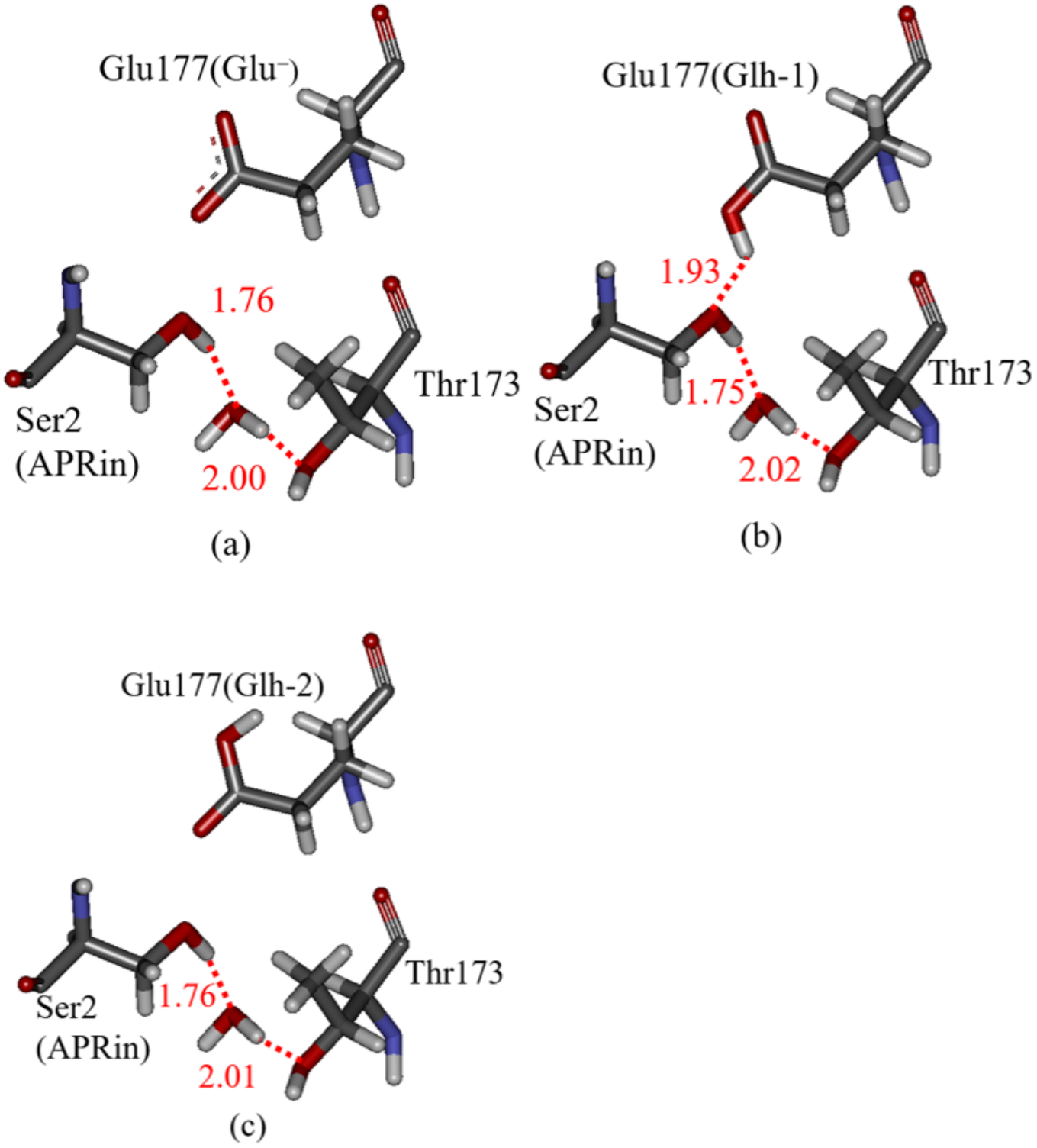

Figure 2

Hydrogen bonding interactions (Å) between the Ser2 of APRin, the Thr173 and Glu177 of APR, and a crystal water molecule in the APR + APRin complex. Glu177 possesses (a) Glu−, (b) Glh-1, and (c) Glh-2 protonation states.

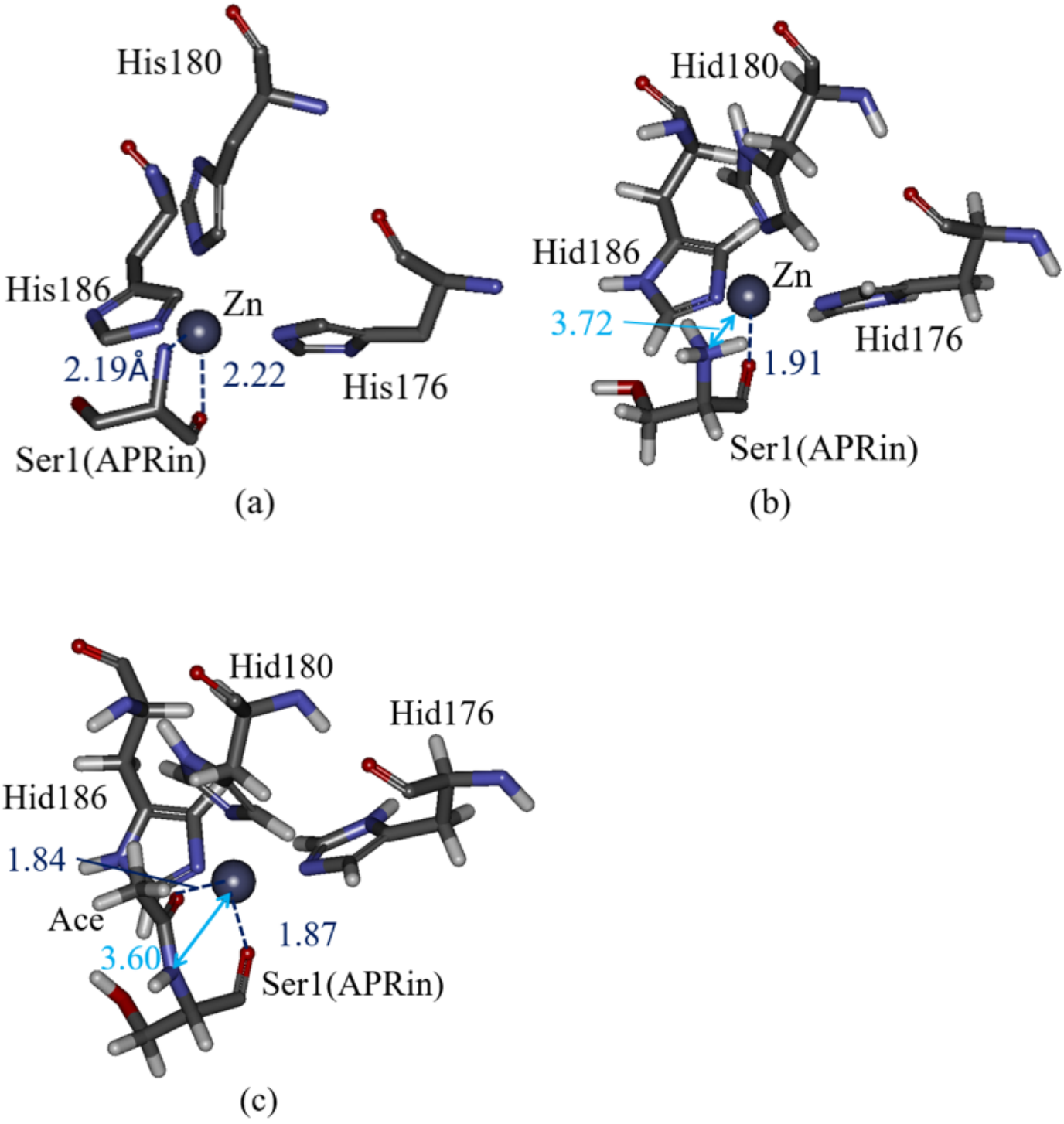

Figure 3

Interaction structures between the Ser1 of APRin and the Zn, Hid176, Hid180, and Hid186 of APR in the APR + APRin complex. (a) The PDB structure (PDB ID: 1JIW) [7] without an H atom. (b) The optimized structure with the NH3+ and COO− terminations of APR and APRin. (c) The optimized structure with the Ace and NMe terminations of APR and APRin. The distances between Zn and some atoms of Ser1 are indicated to clarify the change in structure.

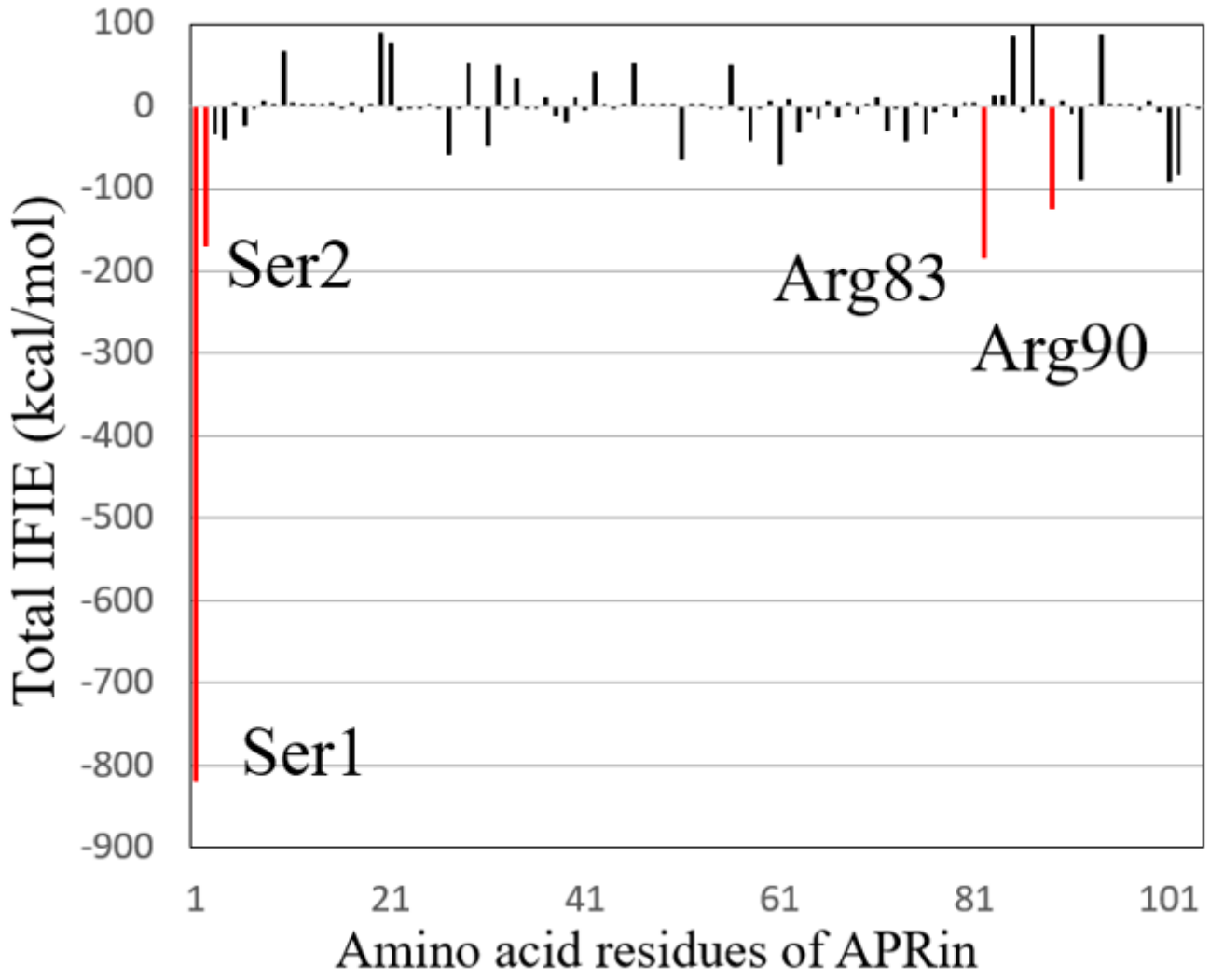

Figure 4

Total IFIEs between each amino acid residue of APRin and all amino acid residues of APR. The APRin residues with total attractive IFIEs greater than 100 kcal/mol are shown in red bars, and their numbers are indicated.

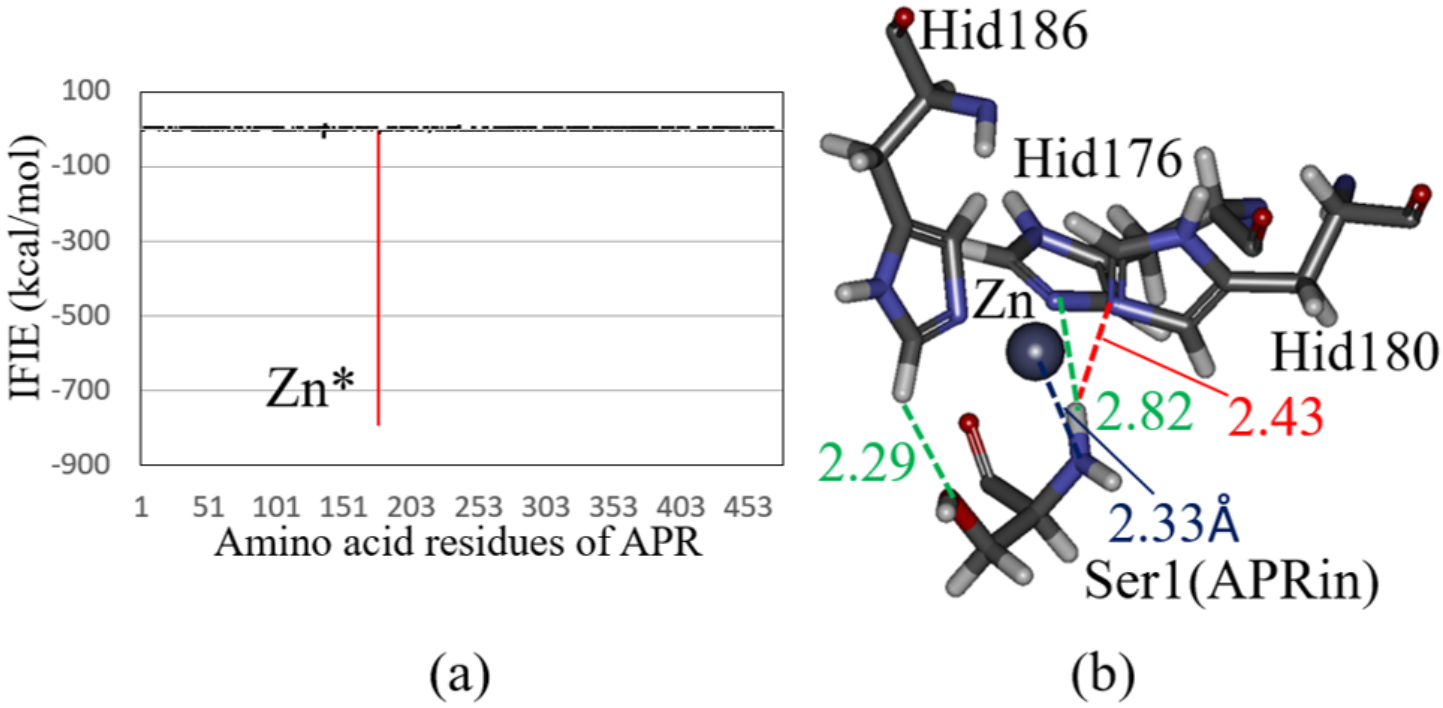

Figure 5

(a) IFIEs between the Ser1 of APRin and each amino acid residue of APR. (b) Interaction structure between the Ser1 and Zn* group (Hid176, Hid180, Hid186, and Zn ion) of APR. The red, green, and blue dashed lines indicate the hydrogen bond between the N-terminal of Ser1 and Hid180 side chain, the electrostatic interactions between Ser1 and the APR residues, and the coordination bond (2.33 Å) between Ser1 and Zn ion, respectively.

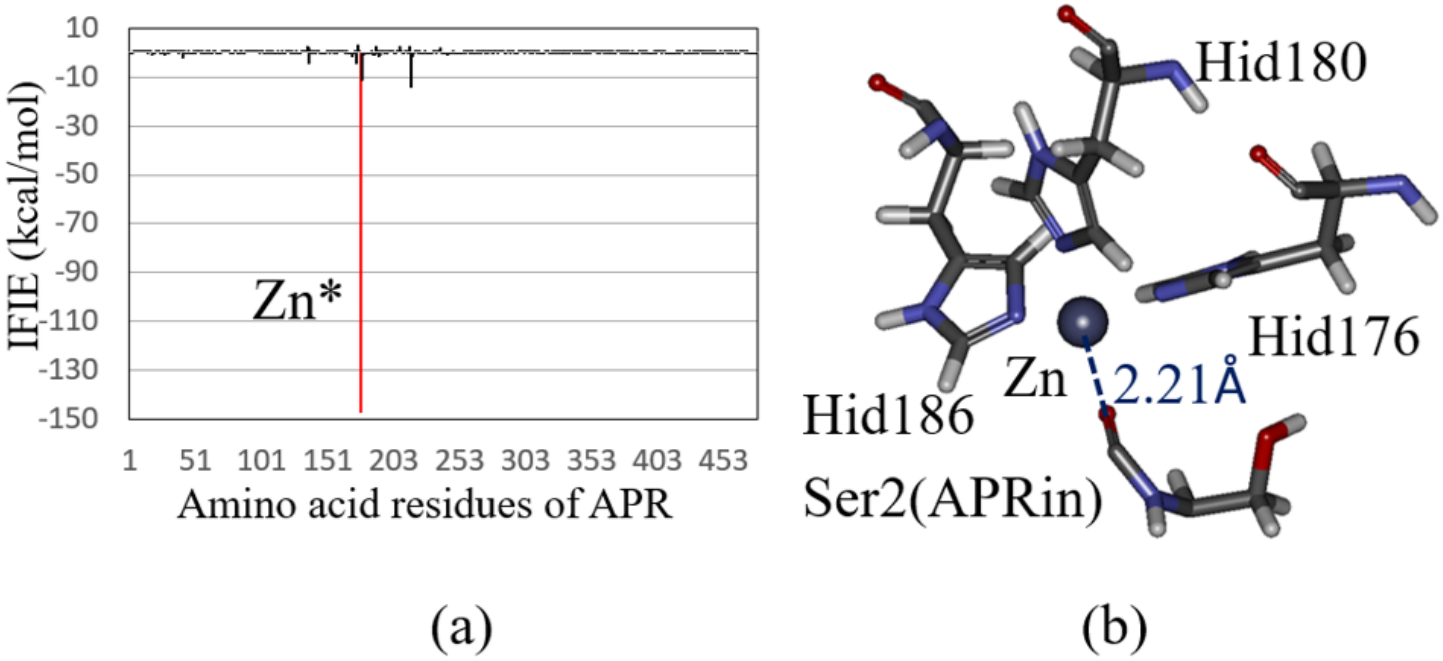

Figure 6

(a) IFIEs between the Ser2 of APRin and each amino acid residue of APR. (b) Interaction structure between the Ser2 and Zn* group (Hid176, Hid180, Hid186, and Zn ion) of APR. The blue dashed line indicates the coordination bond (2.21 Å) between Ser2 and Zn ion.

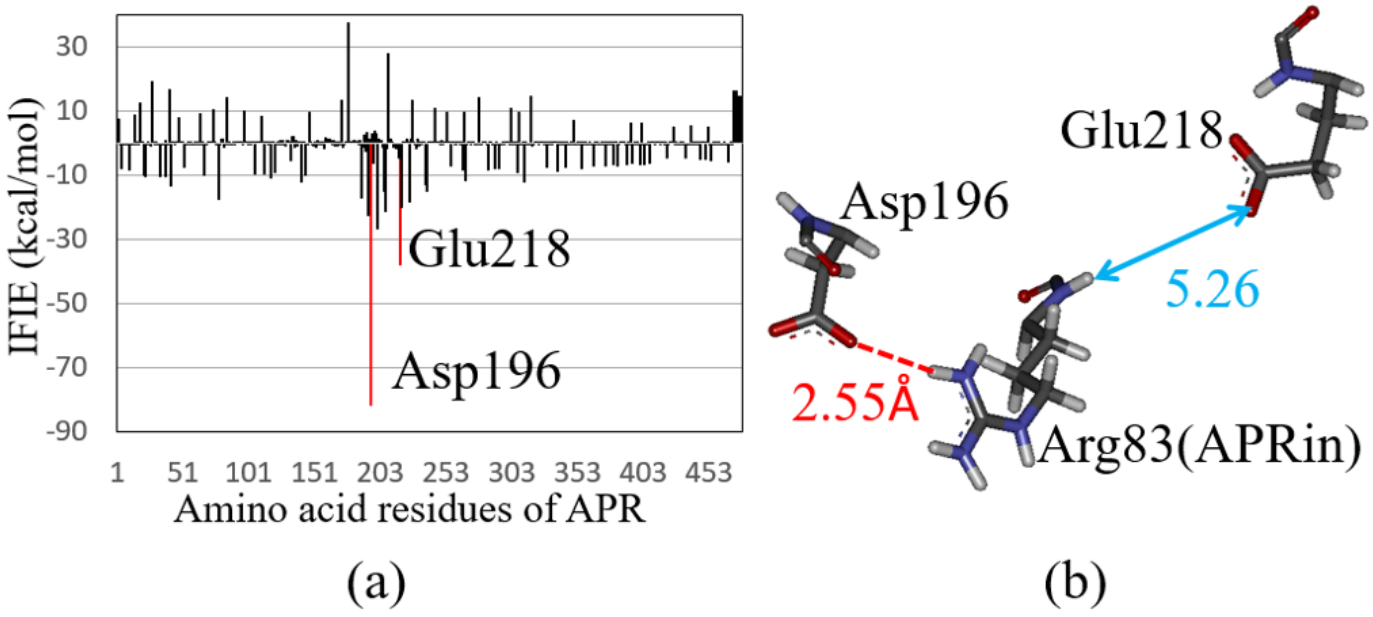

Figure 7

(a) IFIEs between the Arg83 of APRin and each amino acid residue of APR. (b) Interaction structure between the Arg83, Asp196, and Glu218 of APR. The red dashed line indicates the hydrogen bond, and the nearest distance between Arg83 and Glu218 is also shown.

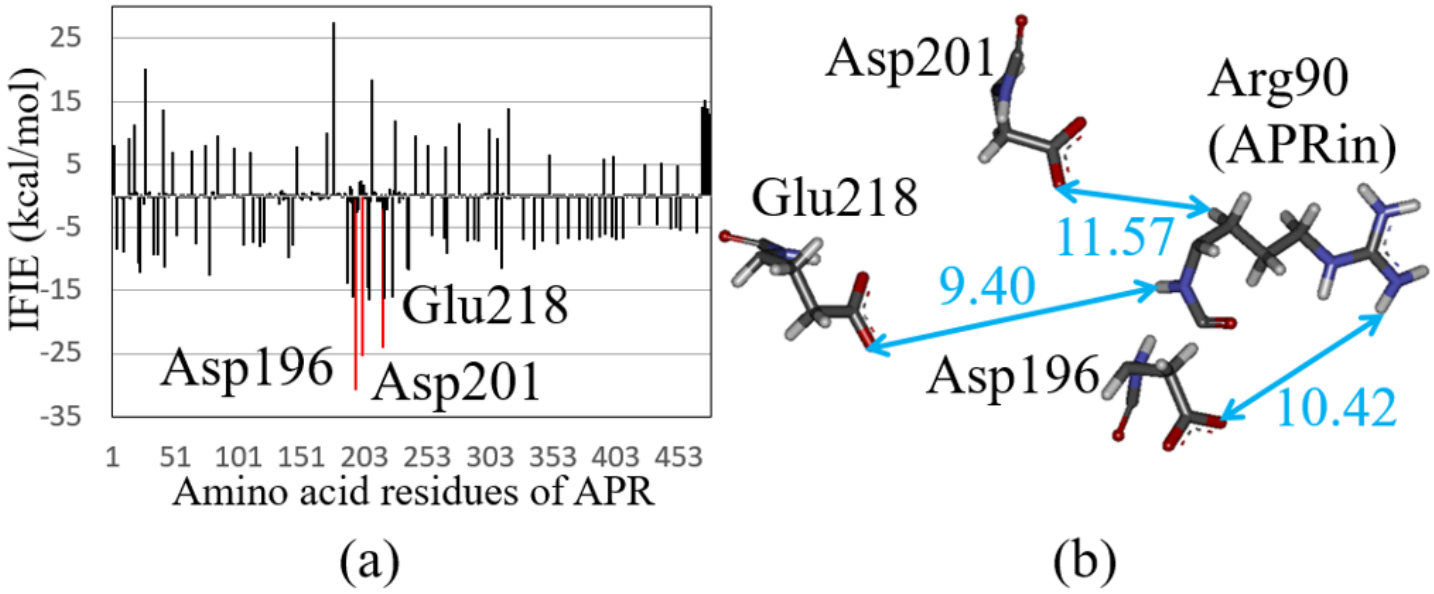

Figure 8

(a) IFIEs between the Arg90 of APRin and each amino acid residue of APR. (b) Interaction structure between Arg90 and the Asp196, Asp201, and Glu218 of APR. There is no direct interaction between Arg90 and these APR residues. The nearest distances between them are shown.

Supplementary Files

This is a list of supplementary files associated with this preprint. Click to download.

- Graphicalabstract.doc
- KuritaSupplementary.docx